L. Barker, S. M. Paul, *Science* **232**, 1004 (1986); K. W. Gee, *Mol. Neurobiol.* **2**, 291 (1988); G. Puia *et al.*, *Neuron* **4**, 759 (1990).
17. M. Orchinik and F. L. Moore, *Soc. Neurosci. Abstr.* **15**, 759 (1989); manuscript in preparation.
18. K. W. Gee, W.-C. Chang, R. E. Brinton, B. S. McEwen, *Eur. J. Pharmacol.* **136**, 419 (1987); N. L. Harrison, M. D. Majewska, J. W. Harrington, J. L. Barker, *J. Pharmacol. Exp. Ther.* **241**, 346 (1987); D. M. Turner, R. W. Ransom, J. S.-J. Yang, R. W. Olsen, *ibid.* **248**, 960 (1989); A. L. Morrow, J. R. Pace, R. H. Purdy, S. M. Paul, *Mol. Pharmacol.* **37**, 263 (1990).
19. V. P. Whittaker, in *Handbook of Neurochemistry*, A. Lajtha, Ed. (Plenum, New York, 1969), vol. 2, pp. 327–364.
20. M. Satre and P. V. Vignais, *Biochemistry* **13**, 2201 (1974); E. N. Cozza, M. F. Foecking, C. E. Gomez-Sanchez, *J. Steroid Biochem.* **35**, 511 (1990); M. V. Leshchenko and P. V. Sergeyev, *Farmakol. Toksikol. (Moscow)* **3**, 60 (1987).
21. Synaptosomes, mitochondria, and nuclei were prepared from fresh brains as described (*19*). The crude cytosolic fraction resulted from a centrifugation of the initial homogenate at 48,000*g* for 45 min. All fractions were resuspended in assay buffer to a protein concentration of 600 μg/ml.
22. We incubated P2 fraction resuspensions with 0.5 nM [^{3}H]QNB ± 10 μM scopalamine to determine nonspecific binding.
23. R. Feyereisen, G. D. Baldridge, D. E. Farnsworth, *Comp. Biochem. Physiol.* **82B**, 559 (1985).
24. The greater enrichment of [^{3}H]CORT binding in the mitochondrial fraction relative to [^{3}H]QNB suggests there may be binding sites for CORT in neuronal mitochondria as well as in synaptic membranes.
25. Thaw-mounted 25-μm brain sections were incubated for 30 min at 22°C with assay buffer containing dexamethasone and ZK91587 (200 nM), then incubated for 2 hours with [^{3}H]CORT (2 nM) in buffer containing dexamethasone and ZK91587 (200 nM). Nonspecific binding was determined in alternate sections by the addition of CORT (10 μM). The reaction was terminated by two 3-min washes in ice-cold buffer. Sections were dried under cool air, apposed to ^{3}H-sensitive film for 2 months, and stained with toluidine blue for histology. The autoradiogram was analyzed by computer-assisted densitometry (DUMAS). Specific binding was determined by subtraction of nonspecific binding from the aligned total binding sections.
26. Adult male *Taricha* in breeding condition were collected locally and experiments were conducted in the field. Males (mean weight, 22 g) received intraperitoneal injections (0.1 ml) of steroid or vehicle (amphibian Ringers with 8% ethanol–2% dimethyl sulfoxide). Testing was initiated 5 min after injection, when stimulus females were added to tanks holding males. Males displaying sexual behavior (dorsal amplectic clasping of female) were removed from tanks. Females received 500 μg of progesterone by injection 24 hours before tests to enhance attractivity [F. L. Moore, *Copeia* **3**, 530 (1978)].
27. L. E. Limbird, *Cell Surface Receptors: A Short Course on Theory and Methods* (Nijhoff, Boston, 1986), pp. 60–94; G. A. Weiland and P. B. Molinoff, *Life Sci.* **29**, 313 (1981).
28. CORT induces sexual behavior in female rats within 5 min of intravenous injection through unknown mechanisms [C. Kubli-Garfias, *Horm. Behav.* **24**, 443 (1990)].
29. R. J. Tallarida and L. S. Jacob, *The Dose-Response Relation in Pharmacology* (Springer-Verlag, New York, 1979), pp. 107–109.
30. We thank A. Blaustein, D. Crews, P. Deviche, K. Moore, C. Propper, and K. Yamamoto for helpful criticisms of the manuscript. For assistance in the field, we thank C. Lowry, L. McKinney, J. Morgan, M. Schroeder, J. Tacchini, B. Ford, and D. Desonie. This work supported by NSF grants BNS-8901500 (F.L.M. and M.O.) and BNS-8909173 (F.L.M.). M.O. was supported by an NSF graduate fellowship.

8 January 1991; accepted 25 March 1991

An Analog of Myristic Acid with Selective Toxicity for African Trypanosomes

TAMARA L. DOERING,* JAYNE RAPER, LAURENCE U. BUXBAUM, STEVEN P. ADAMS, JEFFREY I. GORDON, GERALD W. HART, PAUL T. ENGLUND

***Trypanosoma brucei*, the protozoan parasite responsible for African sleeping sickness, evades the host immune response through the process of antigenic variation. The variant antigen, known as the variant surface glycoprotein (VSG), is anchored to the cell surface by a glycosyl phosphatidylinositol (GPI) structure that contains myristate (*n*-tetradecanoate) as its only fatty acid component. The utilization of heteroatom-containing analogs of myristate was studied both in a cell-free system and in vivo. Results indicated that the specificity of fatty acid incorporation depends on chain length rather than on hydrophobicity. One analog, 10-(propoxy)decanoic acid, was highly toxic to trypanosomes in culture although it is nontoxic to mammalian cells.**

THE EFFECTS OF AFRICAN TRYPANOSOMIASIS on human health and on livestock production are crippling (*1*). Of the 50 million people at risk for sleeping sickness, fewer than 20% have access to protection from, or treatment for, this frequently lethal illness. In addition, the only drug widely used to combat late-stage (meningoencephalitic) disease, melarsoprol, causes fatal side effects in up to 5% of those treated (*2*). There is thus a need for new approaches to chemotherapy and for the design of less toxic drugs. One general approach to drug development is to examine the pathogenic organism for features not shared with its host, in the hope of exploiting these differences to generate selectively toxic agents.

The attachment of surface proteins to eukaryotic cell membranes via GPI structures has been described only in the last few years (*3, 4*). The trypanosome VSG is the best characterized protein of this type, and it differs from mammalian GPI-anchored proteins in containing exclusively myristate (14:0, a fully saturated 14-carbon fatty acid) in its GPI moiety (Fig. 1A) (*5*). During VSG biosynthesis, the anchor is preformed as a GPI called glycolipid A (*6*) [or P2 (*7*)], to which the COOH-terminus of the polypeptide is later attached. The pathway of GPI biosynthesis in trypanosomes has been elucidated by means of a cell-free system (*8–10*) capable of forming glycolipid A. In the presence of uridine 5′-diphosphate–*N*-acetylglucosamine (UDP-GlcNAc) and guanosine 5′-diphosphate–mannose (GDP-Man), the glycan portion of this GPI is constructed de novo on endogenous phosphatidylinositol (PI), producing glycolipid A′ (*8*). This GPI contains two fatty acids more hydrophobic than myristate [one of which is stearate (18:0)], which are sequentially replaced by myristate via a process termed fatty acid remodeling (*10*). First, glycolipid A′ is deacylated to form glycolipid θ, a lyso intermediate. In the presence of myristoyl coenzyme A (CoA), myristate is added to glycolipid θ to form glycolipid A″, with one myristate and one stearate. The final steps in the process involve replacement of the stearate with a second myristate, to form glycolipid A. In the absence of UDP-GlcNAc and GDP-Man, there is no de novo GPI biosynthesis in the cell-free system; however, ^{3}H-labeled myristate is still incorporated into preexisting glycolipid A by a presumed acyl exchange process (*10*).

It is intriguing that the trypanosome anchor strictly requires myristate, particularly because this fatty acid is rare in the GPIs of mammalian proteins (*3*). The specificity is more striking because *T. brucei* lacks the ability to synthesize fatty acids de novo (*11*) and must import these compounds from the infected host's bloodstream. Because mammalian serum contains relatively little myristate [for example, 1 to 2% of fatty acids from total lipids in rat plasma (*12*)], the import process may be quite selective.

To investigate the biological function of the myristoyl moieties of the VSG anchor, we introduced analogs of myristate into the trypanosome system. These fatty acid ana-

T. L. Doering, J. Raper, L. U. Buxbaum, G. W. Hart, P. T. Englund, Department of Biological Chemistry, Johns Hopkins Medical School, Baltimore, MD 21210.
S. P. Adams, Monsanto Company, St. Louis, MO 64167.
J. I. Gordon, Department of Molecular Biology and Pharmacology, Washington University School of Medicine, St. Louis, MO 63110.

*To whom correspondence should be addressed.

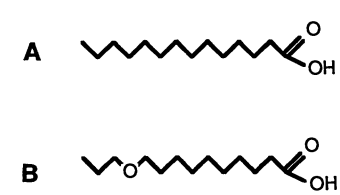

Fig. 1. Structures of myristate (**A**) and O-11 (**B**).

logs, with oxygen substituted for one methylene group (*13*), are similar to myristate with respect to predicted geometry (in solution) but are more hydrophilic. For example, a myristate analog with oxygen substituted for the eleventh carbon (10-(propoxy)decanoic acid, termed O-11) (Fig. 1B) has hydropathic properties similar to those of decanoic acid (10:0) (*13*). These analogs have proved effective in elucidating the biological role of myristate in *N*-myristoyl proteins; analog substitution for myristate dramatically alters the subcellular localization and function of some of these proteins (*14, 15*).

In the trypanosome cell-free system, ^{3}H-labeled O-11 was incorporated into glycolipid A by the acyl exchange reaction even more efficiently than [^{3}H]myristate (Fig. 2A, lanes 2 and 3). Both fatty acids are also incorporated into glycolipid C [a GPI identical to glycolipid A except for an extra fatty acid linked to inositol (*16*)] and into other phospholipids.

In the presence of nonradioactive UDP-GlcNAc and GDP-Man, de novo synthesis of GPI glycans is operative. Subsequent incubation with ^{3}H-labeled fatty acyl CoA results in labeling of both glycolipid A″ [with one myristate (or O-11) and one longer fatty acid] and glycolipid A (*10*). Again, incorporation of [^{3}H]O-11 was slightly more efficient than that of [^{3}H]myristate (Fig. 2A, lanes 4 and 5). Similar results were obtained with two other analogs, 12-(methoxy)dodecanoic acid (O-13) and 5-(octoxy)pentanoic acid (O-6) (*13, 17*).

We then incubated the cell-free system with GDP-[^{3}H]Man and nonradioactive UDP-GlcNAc, to radiolabel early biosynthetic intermediates in the pathway (Fig. 2B, lane 1) (*8*). Further incubation with adenosine triphosphate (ATP), CoA, and myristate drove a fraction of the intermediates through remodeling to completion. Addition of myristate or O-11 yielded comparable amounts of glycolipids A″ and A (Fig. 2B, lanes 4 and 5) (*18*).

These data show that in the cell-free system myristate analogs are incorporated into GPIs at least as efficiently as myristate. In contrast, palmitate, stearate, and an oxygen-substituted analog of palmitate, 12(propoxy)dodecanoic acid, with hydrophobicity comparable to that of myristate, are not utilized by the remodeling process (*17*). It appears, then, that the specificity of fatty acid remodeling depends more on the chain length of incoming fatty acid substrates than on their hydrophobicity.

We also investigated the metabolism of myristate analogs in living trypanosomes. [^{3}H]O-11 is incorporated into numerous lipids, in a pattern similar to that of [^{3}H]myristate (Fig. 3A); the products include O-11 counterparts of glycolipids A and C. These GPIs were identified by comigration with standards on thin layer chromatographs, as well as by susceptibility to specific phospholipases (*19*). For both [^{3}H]O-11 and [^{3}H]myristate, initial labeling of GPI species was rapid and by 20 min had attained steady state (*17*). At steady state, however, incorporation of [^{3}H]O-11 into glycolipids A and C, or into VSG protein (Fig. 3B), was less than 10% of [^{3}H]myristate incorporation. As expected, fatty acid radiolabel is released from VSG when gels are treated with alkali (0.2 M KOH in methanol, 1 hour, room temperature) consistent with ester linkage of [^{3}H]fatty acid to the GPI anchor (*17*). Long exposures of similar gels show minor species (in both lanes) that are not susceptible to alkaline hydrolysis; these could represent radiolabeled, normally *N*-myristoylated pro-

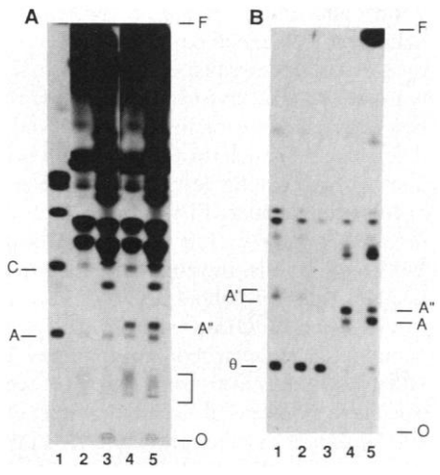

Fig. 2. (**A**) Cell-free radiolabeling of GPI species with [^{3}H]myristoyl CoA and [^{3}H]O-11 CoA. Washed trypanosome lysate (5×10^8 cell equivalents per milliliter) was preincubated (8 min, 37°C) with 1 mM each UDP-GlcNAc and GDP-Man (*24*). [^{3}H]myristoyl CoA or [^{3}H]O-11 CoA (each at 2.5 μM, 31.7 Ci/mmol) was added and incubation continued for 5 min. We prepared the [^{3}H]acyl CoA from [^{3}H]fatty acids, using *Pseudomonas* sp. acyl CoA synthetase (*10*). Samples were extracted in chloroform:methanol:water (10:10:3) and centrifuged, and the supernatant fractions were dried under nitrogen (*8*). To cleave unincorporated [^{3}H]acyl CoA, we boiled samples for 8 min in 1 mM dithiothreitol. After two extractions with water-saturated butanol, the pooled organic extracts were washed with water, and 1.5×10^7 cell equivalents per reaction were analyzed on silica gel 60 thin-layer chromatography plates developed in 10:10:3 solvent (*8*). Lane 1, marker lipids, labeled in vivo with [^{3}H]myristate (*6*); lane 2, incubation with [^{3}H]myristoyl CoA, no preincubation with nucleotide sugars; lane 3, same as lane 2 but with [^{3}H]O-11 CoA; lane 4, incubation with [^{3}H]myristoyl CoA after preincubation with UDP-GlcNAc and GDP-Man to allow de novo GPI glycan synthesis; lane 5, same as lane 4 but [^{3}H]O-11 CoA. In this and the following figures: O, origin; F, solvent front; A, C, and A″, GPI species (see text). The bracket indicates a smear of residual [^{3}H]acyl CoA. (**B**) The effects of myristate and O-11 on GDP-[^{3}H]Man radiolabeled GPI intermediates. Lysate (5×10^8 cell equivalents per milliliter) was first incubated with 1 mM UDP-GlcNAc and 3 μCi/ml GDP-[^{3}H]Man (17 Ci/mmol; 0.18 μM final concentration) for 5 min at 37°C, and then incubated with 1 mM nonradioactive GDP-Man for 3 min at 37°C to allow radiolabel to accumulate in glycolipids A′ and θ (lane 1). To examine fatty acid remodeling, we further incubated the reaction mixture for 5 min with either no additions (lane 2), or with 0.6 mM ATP, 0.2 mM CoA, and the following: lane 3, no fatty acid; lane 4, 1 mM myristate; lane 5, 1 mM O-11 (*13*). Sample extraction and chromatography was as in (A). The prominent band near the front in lane 5 is unidentified; it appears inconsistently.

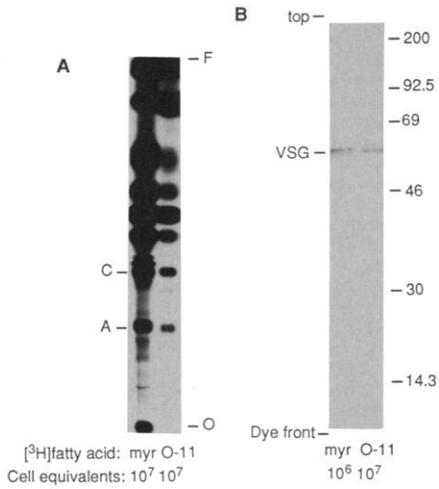

Fig. 3. (**A**) Incorporation of [^{3}H]myristate and [^{3}H]O-11 into living trypanosomes. Cloned IL-Tat 1.3 trypanosomes, isolated from mouse blood (*25*), were washed once in minimum essential medium (MEM) "alpha" (catalog number 320-2561 AJ, Gibco, Grand Island, New York) supplemented with glucose (4.4 g/liter), thymidine (3.9 mg/liter), hypoxanthine (13.6 mg/liter), phenylalanine (68 mg/liter), tyrosine (64 mg/liter), essentially fatty acid–free bovine serum albumin (BSA) (10 g/liter) (Sigma, St. Louis, Missouri), pyruvate (110 mg/liter), penicillin (50,000 units/liter), streptomycin (50 mg/liter), and 5% fetal calf serum. Cells were suspended in the same medium (5×10^7 cells/ml) with 100 μCi/ml [^{3}H]myristic acid (New England Nuclear, 32 Ci/mmol) or [^{3}H]O-11 (32 Ci/mmol), incubated at 37°C for 80 min, and washed. Glycolipids were extracted from 10^7 cells (*26*) and analyzed by thin layer chromatography as in Fig. 2. Abundant species above glycolipid C are cellular lipids (*27*). Myr, myristate; A, glycolipid A; C, glycolipid C. (**B**) Incorporation of [^{3}H]myristate and [^{3}H]O-11 into VSG. Cells labeled as in (A) (10^8 cells/ml, 90 min) were washed twice and boiled in 20 μl of SDS–polyacrylamide gel electrophoresis sample buffer. Protein from cells labeled with [^{3}H]myristate (10^6 cell equivalents) or [^{3}H]O-11 (10^7 cell equivalents) was analyzed by electrophoresis on an 11% polyacrylamide gel and fluorographed (scale in kilodaltons).

teins (*17*). Two other myristate analogs, [^{3}H]O-6 and [^{3}H]O-13, demonstrated similar kinetics and product profile but were incorporated into glycolipids to an even lesser extent at steady state [1 to 3% of the myristate level (*17, 20*)].

The inefficient in vivo incorporation of analogs (compared to myristate) contrasts sharply with incorporation in the cell-free system, where analogs and myristate are handled similarly. Because the cell-free data demonstrate that discrimination does not occur at the level of the fatty acid remodeling enzymes, factors dependent on cell integrity (such as fatty acid uptake, metabolic processing, or compartmentalization) are probably responsible for the difference. Consistent with this idea, trypanosomes in culture accumulated eight times more myristate than O-11 (*17*).

In its fatty acid remodeling mechanism, the trypanosome has evolved a unique and highly efficient mechanism for incorporating myristate into GPIs. Because this myristate could play a crucial role in trypanosomal biology, we studied the effects of O-11 and other myristate analogs on the viability of this parasite in culture. At a concentration of 10 μM, O-11 had a striking effect, killing most trypanosomes in a few hours (Fig. 4A) (*21*). The median lethal dose (LD_{50}) of O-11 was less than 1 μM (inset, Fig. 4A). At 10 μM, O-13 inhibited trypanosome growth by about 40%; O-6 only inhibited growth by 10% (*17*).

O-11 is not generally cytotoxic. For example, 100 μM O-11 has no effect on growth, viability, or DNA and protein synthesis of human T lymphoid cells (*22*); similarly, 100 μM O-11 does not affect *Saccharomyces cerevisiae* (*14*). To examine the specificity of the O-11 toxicity to parasites, we tested it on cultured procyclic trypanosomes (the developmental form of *T. brucei* found in the tsetse fly vector). Instead of VSG, procyclics express a GPI-linked surface antigen (procyclic acidic repetitive protein or procyclin), which does not contain myristate (*23*). O-11 (10 μM) did not affect procyclic growth in culture (Fig. 4B). At 50 μM, O-11 decreased the growth rate of procyclic trypanosomes by 50%, but myristate at that concentration had the same effect (*17*).

Treatment with O-11 was associated with gross alterations in trypanosome morphology (Fig. 5, compare A and B). As early as 3 hours after incubation with 10 μM O-11 some cells appeared unhealthy: motility was reduced, integrity of shape was lost, and vacuolar inclusions appeared. These effects increased with time of culture, until by 8 hours nearly all cells were nondividing, distorted by large vacuoles, and barely motile. Lower concentrations of O-11 that still inhibited trypanosome growth also induced these effects but over a longer time period. However, even after 45 hours of treatment with 10 μM O-11, occasional cells (fewer than 1%) still appeared normal.

We examined the integrity of the trypanosome surface coat, composed of VSG, by electron microscopy. No difference in coat morphology was observed between cells treated with O-11 and those treated with myristate, although the cells appeared distorted (Fig. 5, C through F). Treated cells developed massive vacuolar structures, which exhibited on their inner surface the VSG coat typically found on the outer sur-

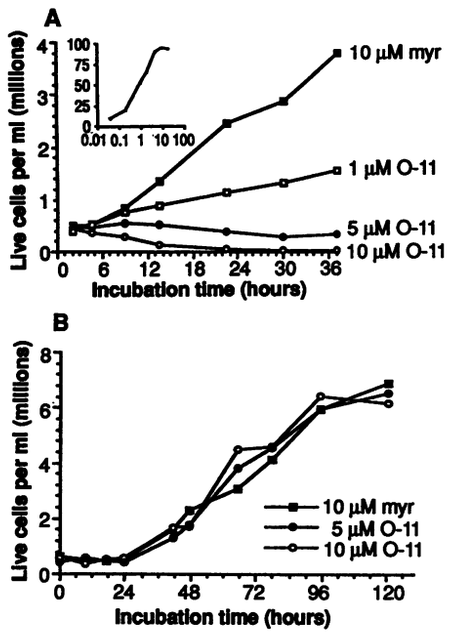

Fig. 4. Effect of O-11 on (**A**) cultured bloodstream form and (**B**) procyclic trypanosomes. Bloodstream forms of *T. brucei* strain 427 (variant 221). Trypanosomes were isolated from mouse blood at a parasitemia of 5×10^8 cells/ml (*25*) and cultured (37°C, 5% CO_2) in prewarmed medium (as in Fig. 2) containing 40 μM monothioglycerol (*28*) and myristate (myr) or O-11 as indicated. Similar growth curves were seen in five independent experiments. Procyclic trypanosomes: Strain TREU 667 was cultured at 28°C in SM medium (*29*). The inset dose response curve shows the percentage of cells killed at 25 hours as a function of O-11 concentration (micromolar, in log scale); these data are compiled from five experiments. Means of duplicate counts (generally within 10%) are shown, with any cell demonstrating minimal movement scored as "live." Myristate or O-11 (*13*) was added from a 1000× stock in absolute ethanol; growth curves of control cultures (0.1% ethanol) were indistinguishable from those of the cultures containing 10 μM myristate.

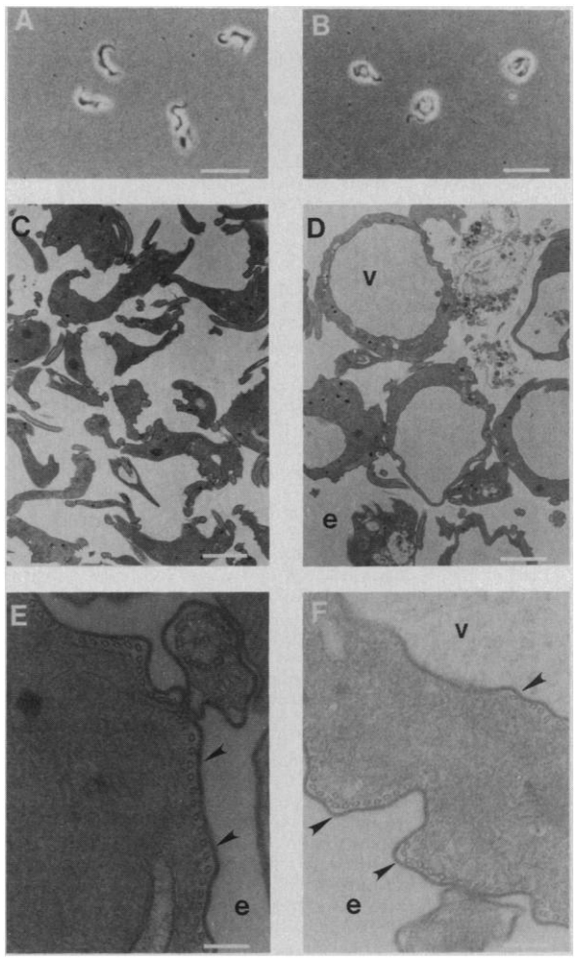

Fig. 5. Bloodstream form trypanosomes were cultured for 24 hours in the presence of 10 μM myristate (**A**, **C**, and **E**) or 5 μM O-11 (**B**, **D**, and **F**). (A) and (B) are phase micrographs photographed on a Zeiss Axiophot instrument. Bar, 15 μm. (C) through (F) are cells prepared for electron microscopy according to the procedure described by Cross (*30*). Bar, C and D, 2.1 μm; E and F, 0.2 μm; v, vacuole; e, extracellular medium; arrowheads indicate VSG layer.

face of trypanosomes. Like the trypanosome surface membrane, the vacuolar membrane had underlying microtubules (Fig. 5F). The origin of these structures is unknown, but it may involve membrane transport or targeting.

The toxicity of O-11 for bloodstream trypanosomes may be related to the metabolism or function of the VSG GPI, especially because similar concentrations do not affect the growth and viability of procyclic trypanosomes. However, our experiments cannot rule out the possibility that toxicity is mediated by alteration of *N*-myristoylated proteins or by some change in membrane structure. The latter could be caused by incorporation of analog into phospholipids as well as into VSG. Whatever the mechanism of toxicity, these studies suggest a new approach to antitrypanosome chemotherapy.

REFERENCES AND NOTES

1. C. Laitman, *Trop. Dis. Res. News* **31**, 3 (1990).
2. S. L. Hajduk, P. T. Englund, D. H. Smith, in *Tropical and Geographic Medicine*, K. S. Warren and A. A. F. Mahmoud, Eds. (McGraw-Hill, New York, 1989), pp. 268–281; *Tropical Disease Research: Science at Work* (World Health Organization, Geneva, Switzerland, 1986).
3. G. A. M. Cross, *Annu. Rev. Cell Biol.* **6**, 1 (1990); T. L. Doering, W. J. Masterson, G. W. Hart, P. T. Englund, *J. Biol. Chem.* **265**, 611 (1990); M. G. Low and A. R. Saltiel, *Science* **239**, 268 (1988); J. R. Thomas, R. A. Dwek, T. W. Rademacher, *Biochemistry* **29**, 5413 (1990).
4. M. A. J. Ferguson and A. F. Williams, *Annu. Rev. Biochem.* **57**, 285 (1988).
5. M. A. J. Ferguson and G. A. M. Cross, *J. Biol. Chem.* **259**, 3011 (1984).
6. J. L. Krakow, D. Hereld, J. D. Bangs, G. W. Hart, P. T. Englund, *ibid.* **261**, 12147 (1986).
7. A. K. Menon, S. Mayor, M. A. J. Ferguson, M. Duszenko, G. A. M. Cross, *ibid.* **263**, 1970 (1988).
8. W. J. Masterson, T. L. Doering, G. W. Hart, P. T. Englund, *Cell* **56**, 793 (1989).
9. A. K. Menon, R. T. Schwarz, S. Mayor, G. A. M. Cross, *J. Biol. Chem.* **265**, 9033 (1990).
10. W. J. Masterson, J. Raper, T. L. Doering, G. W. Hart, P. T. Englund, *Cell* **62**, 73 (1990).
11. A. Mellors and A. Samad, *Parasitol. Today* **5**, 239 (1989).
12. H. Dixon, *Trans. R. Soc. Trop. Med. Hyg.* **61**, 12 (1967); D. M. Raben, unpublished observations.
13. R. O. Heuckeroth, L. Glaser, J. I. Gordon, *Proc. Natl. Acad. Sci. U.S.A.* **85**, 8795 (1988).
14. R. O. Heuckeroth and J. I. Gordon, *ibid.* **86**, 5262 (1989).
15. D. R. Johnson *et al.*, *ibid.* **87**, 8511 (1990).
16. J. L. Krakow, T. L. Doering, W. J. Masterson, G. W. Hart, P. T. Englund, *Mol. Biochem. Parasitol.* **36**, 263 (1989); S. Mayor *et al.*, *J. Biol. Chem.* **265**, 6164 (1990); S. Mayor, A. K. Menon, G. A. M. Cross, *ibid.*, p. 6174.
17. T. L. Doering, L. U. Buxbaum, J. Raper, unpublished observations.
18. The CoA derivative of O-11 (and of O-6 and O-13) is synthesized in the cell-free system as readily as that of myristate (*17*).
19. Glycolipid A and its [^{3}H]O-11–labeled counterpart are cleaved by PI-PLC from *Bacillus thuringiensis*, GPI-PLC from *T. brucei*, and GPI-PLD from human serum; glycolipid C and its counterpart only by GPI-PLD (PLC, phospholipase C; PLD, phospholipase D). Conditions were as in (*8*).
20. All analogs and myristate were adjusted to the same specific radioactivity throughout.
21. Mass analysis showed that after 6 hours of culture with 10 μM O-11 4% of the fatty acids on trypanosome VSG were O-11, affecting up to 8% of the VSG molecules (*17*).
22. M. L. Bryant, R. O. Heuckeroth, J. T. Kimata, L. Ratner, J. I. Gordon, *Proc. Natl. Acad. Sci. U.S.A.* **86**, 8655 (1989); M. L. Bryant *et al.*, *ibid.* **88**, 2055 (1991).
23. J. P. Richardson, R. P. Beecroft, D. L. Tolson, M. K. Liu, T. W. Pearson, *Mol. Biochem. Parasitol.* **31**, 203 (1988); C. E. Clayton and M. R. Mowatt, *J. Biol. Chem.* **264**, 15088 (1989).
24. Lysate preparation, washes, and incubation buffers as in (*10*).
25. J. D. Bangs, D. Hereld, J. L. Krakow, G. W. Hart, P. T. Englund, *Proc. Natl. Acad. Sci. U.S.A.* **82**, 3207 (1985).
26. T. L. Doering, W. J. Masterson, P. T. Englund, G. W. Hart, *J. Biol. Chem.* **264**, 11168 (1989).
27. Methanolysis of glycolipids A and C and examination of the resulting fatty acid methyl esters by reverse-phase thin layer chromatography showed that O-11 or myristate incorporated into these GPI species was not metabolized; similar analysis of the other (less polar) labeled lipids showed that they contained both unmodified [^{3}H]O-11 or [^{3}H]myristate as well as species that had been elongated (*17*).
28. B. Hamm, A. Schindler, D. Mecke, M. Duszenko, *Mol. Biochem. Parasitol.* **40**, 13 (1990).
29. I. Cunningham, *J. Protozool.* **24** (no. 2), 325 (1977).
30. G. A. M. Cross, *Parasitology* **71**, 393 (1975).

31. Supported by grants from the National Institutes of Health (AI21334 and AI27179), from the MacArthur Foundation, and from Monsanto Company. T.L.D. and L.U.B. are supported by Medical Scientist Training grant 5T32GM07309. We are grateful to J. Welply (Monsanto Corporation) for suggesting this collaboration. We appreciate M. Delannoy's help with the electron microscopy and T. Ting's and I. Chiu's assistance with phase microscopy. We thank V. Klein and S. Skiles for technical support; M. S. Pessin-Minsley and D. M. Raben for helpful advice; P. Talalay, T. A. B. Shapiro, and K. Mensa-Wilmot for reviewing this manuscript; and J. D. Bangs and W. J. Masterson for discussions. We thank G. A. M. Cross for providing *T. brucei* strain 427 (variant 221). We thank J. Eid and C. Decker for providing trypanosome strain TREU 667.

25 January 1991; accepted 9 May 1991

Reading a Neural Code

WILLIAM BIALEK,* FRED RIEKE,* ROB R. DE RUYTER VAN STEVENINCK,† DAVID WARLAND

Traditional approaches to neural coding characterize the encoding of known stimuli in average neural responses. Organisms face nearly the opposite task—extracting information about an unknown time-dependent stimulus from short segments of a spike train. Here the neural code was characterized from the point of view of the organism, culminating in algorithms for real-time stimulus estimation based on a single example of the spike train. These methods were applied to an identified movement-sensitive neuron in the fly visual system. Such decoding experiments determined the effective noise level and fault tolerance of neural computation, and the structure of the decoding algorithms suggested a simple model for real-time analog signal processing with spiking neurons.

ALL OF AN ORGANISM'S INFORMATION about the sensory world comes from real-time observation of the activity of its own neurons. Incoming sensory information is represented in sequences of essentially identical action potentials, or "spikes." To understand real-time signal processing in biological systems, one must first understand this representation: Does a single neuron signal only discrete stimulus "features," or can the spike train represent a continuous, time-varying input? How much information is carried by the spike train? Is the reliability of the encoded signal limited by noise at the sensory input or by noise and inefficiencies in the subsequent layers of neural processing? Is the neural code robust to errors in spike timing? Clear experimental answers to these questions have been elusive (*1, 2*). We present an approach to the characterization of the neural code that provides explicit and sometimes surprising answers to these questions.

The first recordings from single sensory neurons demonstrated that the intensity of a static stimulus can be coded in the firing rate of a sensory neuron (*3*). This concept of rate coding, extended to time-dependent stimuli, provides the framework for most studies of neural coding, leading to the definition of receptive fields, temporal filter characteristics, and so on. Beyond rate coding, a variety of different statistical measures have been proposed—interval distributions, correlation functions, and so forth (*1, 4*). As with the rate itself, these quantities can be seen as moments of the probability distribution $P[\{t_i\}|s(\tau)]$ that describes the likelihood of different spike trains $\{t_i\}$, given the stimulus $s(\tau)$ (*5*). These moments, however, are not properties of a single spike train; they are average properties of an ensemble of spike trains (*6*). Organisms rarely have the opportunity to compute these averages: To say that information is coded in firing rates is of no use to the organism unless one can

W. Bialek, F. Rieke, D. Warland, Department of Physics and Department of Molecular and Cell Biology, University of California, Berkeley, Berkeley, CA 94720.
R. R. de Ruyter van Steveninck, Department of Biophysics, Rijksuniversiteit Groningen, the Netherlands.

*Present address, NEC Research Institute, 4 Independence Way, Princeton, NJ 08540.
†Present address, Department of Audiology, University Hospital, P.O. Box 30.001, 9700 RB, Groningen, the Netherlands.